Muscle myosins form folded monomers, dimers, and tetramers during filament polymerization in vitro

Xiong Liu[a,1], Shi Shu[a], and Edward D. Korn[a,1]

[a]Laboratory of Cell Biology, Cell and Developmental Biology Center, National Heart, Lung, and Blood Institute, National Institutes of Health, Bethesda, MD 20892

Contributed by Edward D. Korn, May 14, 2020 (sent for review February 3, 2020; reviewed by Sandra Citi and James A. Spudich)

Muscle contraction depends on the cyclical interaction of myosin and actin filaments. Therefore, it is important to understand the mechanisms of polymerization and depolymerization of muscle myosins. Muscle myosin 2 monomers exist in two states: one with a folded tail that interacts with the heads (10S) and one with an unfolded tail (6S). It has been thought that only unfolded monomers assemble into bipolar and side-polar (smooth muscle myosin) filaments. We now show by electron microscopy that, after 4 s of polymerization in vitro in both the presence (smooth muscle myosin) and absence of ATP, skeletal, cardiac, and smooth muscle myosins form tail-folded monomers without tail–head interaction, tail-folded antiparallel dimers, tail-folded antiparallel tetramers, unfolded bipolar tetramers, and small filaments. After 4 h, the myosins form thick bipolar and, for smooth muscle myosin, side-polar filaments. Nonphosphorylated smooth muscle myosin polymerizes in the presence of ATP but with a higher critical concentration than in the absence of ATP and forms only bipolar filaments with bare zones. Partial depolymerization in vitro of nonphosphorylated smooth muscle myosin filaments by the addition of MgATP is the reverse of polymerization.

muscle myosins | polymerization | electron microscopy

Based on their sequences and filament structures, muscle myosin 2 (MM2) can be divided into skeletal, cardiac, and smooth muscle myosins (1). MM2 monomers have two identical heavy chains (HC) of ∼2,000 amino acid residues and two pairs of regulatory light chains (RLCs) and essential light chains (ELCs) of ∼150–170 residues. The N-terminal ∼780 residues of each HC fold into a globular head that contains a motor domain with F-actin–activated MgATPase activity. One RLC and ELC bind to each HC downstream of the head, forming the neck (lever arm), and the remaining C-terminal residues of the two HCs dimerize into a long coiled-coil helical tail.

Since the ground-breaking papers by Huxley (2, 3), synthetic filaments of skeletal muscle myosin (SkM2) and cardiac myosin (CaM2) have been described as bipolar structures with oppositely oriented clusters of myosin heads at the two ends of the filament and a central bare zone. Filaments of smooth muscle myosin (SmM2) are generally considered to be side-polar with oppositely oriented heads on different sides of the filament rather than at the filament ends (4, 5). However, synthetic SkM2 filaments with only a few or no detectable bare zones (5–8) and synthetic SmM2 bipolar filaments with bare zones (4, 5, 9) have been reported.

Monomers of nonphosphorylated SmM2 and nonmuscle myosin 2 (NM2) exist in two conformations—an extended conformation, 6S (its sedimentation coefficient), in the absence of ATP and, in the presence of ATP, a compact 10S conformation. In the 10S monomer, the coiled-coil tail is folded into three approximately equal segments and the two heads associate with each other (interacting-head motif, IHM), with the RLC and the first segment (S2) of the folded tail (10–12). Phosphorylation of the RLC shifts the monomer equilibrium in the presence of ATP toward unfolded 6S monomers (13). The 10S structure differs from the IHM conformation, which does not require a folded tail or head–tail interaction, and which can occur on filaments as well as monomers (14–16).

It had been assumed that the 10S monomers of SmM2 and NM2 are polymerization incompetent (17, 18) and that only 6S monomers polymerize into filaments (18). However, we recently determined (19, 20) that polymerization in vitro of both RLC-phosphorylated and RLC-unphosphorylated NM2s, in both the presence and absence of ATP, most likely proceeds from monomers with folded tails to antiparallel folded-tail dimers and tetramers that unfold and assemble into bipolar filaments.

Although this polymerization pathway is contrary to that generally assumed for muscle myosins, Trybus and Lowey (21) had observed that folded SmM2 monomers can be in equilibrium with SmM2 polymers and form folded antiparallel dimers and suggested that filament assembly might proceed via the association of folded monomers. Also, more than 20 y ago. it was observed that folded monomers were in equilibrium with SkM2 and CaM2 filaments under physiological conditions in vitro (22–24) and in human smooth muscle cells (25). To the best of our knowledge, folded antiparallel tetramers have not been reported for any muscle myosin either in vitro or in vivo.

We have now investigated potential intermediates in the in vitro polymerization of SkM2, CaM2, and SmM2 utilizing the same experimental procedure we used to determine intermediates in the in vitro polymerization of NM2s, i.e., negative staining electron microscopy of glutaraldehyde-fixed samples after polymerization for just 4 s (20).

Significance

Muscle myosins polymerize into thick filaments that drive muscle contraction by interaction with actin thin filaments. The details of muscle myosin polymerization into thick filaments are not known. Current hypotheses are that elongated myosin monomers form antiparallel dimers that polymerize into filaments. However, we find polymerization in vitro of skeletal, cardiac, and smooth muscle myosins involves formation of monomers with folded tails, tail-folded dimers, and tail-folded tetramers. These observations should stimulate studies of the pathway of formation of muscle myosins in vitro and in vivo including the possible roles of the multiple myosin-associated proteins on in vivo polymerization.

Author contributions: X.L. and E.D.K. designed research; X.L. and S.S. performed research; X.L., S.S., and E.D.K. analyzed data; and X.L. and E.D.K. wrote the paper.

Reviewers: S.C., University of Geneva; and J.A.S., Stanford University School of Medicine.

The authors declare no competing interest.

[1]To whom correspondence may be addressed. Email: liux@nhlbi.nih.gov or edk@nih.gov.

This article contains supporting information online at https://www.pnas.org/lookup/suppl/doi:10.1073/pnas.2001892117/-/DCSupplemental.

First published June 22, 2020.

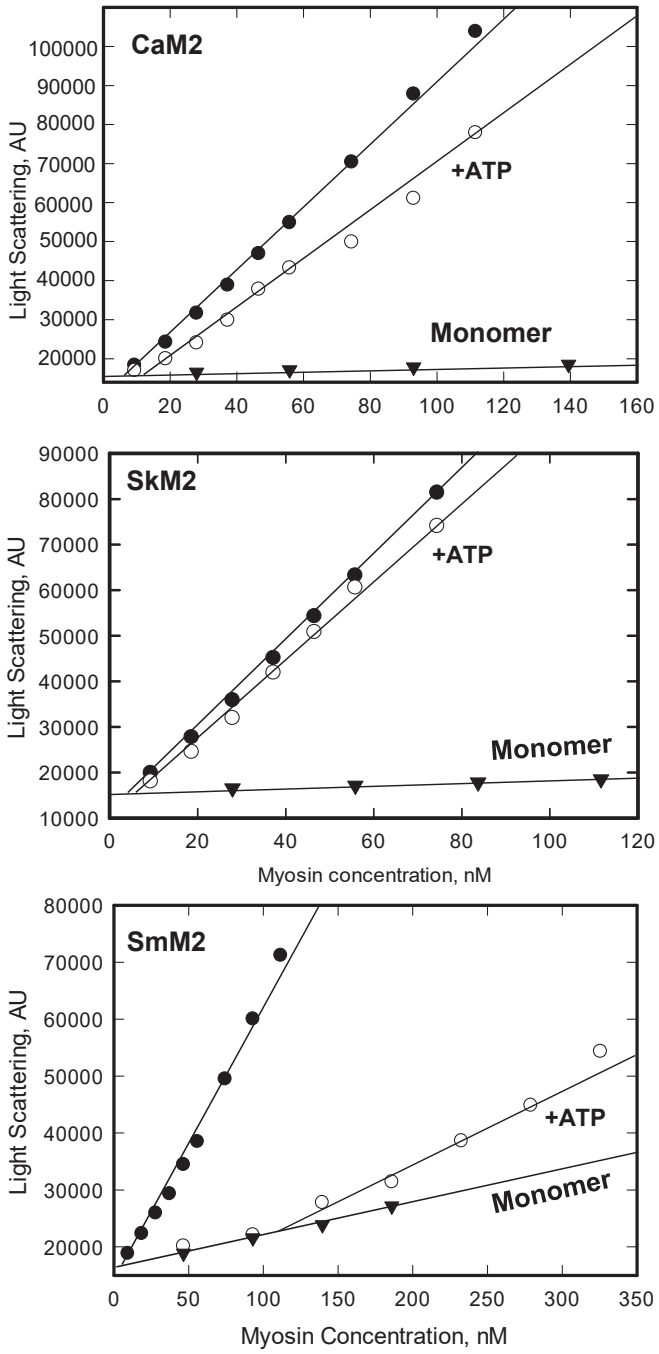

Fig. 1. Light scattering as a function of the concentrations of CaM2, SkM2, and SmM2 polymerized for overnight with (○) and without (•) ATP. The intersections of the curves for the polymerized myosins and myosin monomers (▼) are the critical polymerization concentrations. Note that the scale of the *x* axis is different for SmM2 than for CaM2 and SkM2. Data points are the average of at least two independent experiments.

Results

Non-RLC–Phosphorylated SmM2 Polymerizes in the Presence of ATP. First, we assayed the polymerization of SkM2, CaM2, and non-RLC phosphorylated SmM2 by light scattering in the absence and presence of ATP. In the absence of ATP, all three myosins polymerized with similar slopes of light scattering as a function of myosin concentration (Fig. 1). Addition of ATP to the polymerization buffer did not significantly affect the light scattering slopes of SkM2 and CaM2 but substantially decreased the light scattering slope of SmM2 (Fig. 1). The critical concentrations of SkM2 and CaM2 were minimally affected by ATP in the polymerization buffer—6 and 13 nM in the presence of ATP and 4 and 7 nM in the absence of ATP (Fig. 1). However, the critical concentration of SmM2 was substantially higher in the presence of ATP, 117 nM, than in the absence of ATP, 6 nM (Fig. 1).

CaM2 and SkM2 formed filaments both with bare zones (~20%) but mostly without bare zones (~80%) when polymerized for 4 h in the presence or absence of ATP (Figs. 2–4). Consistent with the light scattering data (Fig. 1), unphosphorylated SmM2 polymerized for 4 h in the presence of ATP formed fewer and smaller filaments than SmM2 polymerized in the absence of ATP (Figs. 2–4 and Table 1). When polymerized for 4 h in the absence of ATP, SmM2 formed bipolar filaments with (~55%) and without (~20%) bare zones and side-polar filaments (~25%) but formed only bipolar filaments with long bare zones (Fig. 4 and Table 1) when polymerized in the presence of ATP (Fig. 4 and Table 1). ATP caused significant difference in filament type for SmM2 but not for SkM2 and CaM2 (Fig. 4). Again, consistent with the light scattering, the filaments of SmM2 polymerized with ATP were substantially smaller than these polymerized in the absence of ATP (Table 1).

Formation of Folded Monomers, Dimers, and Tetramers. Glutaraldehyde was added within ~4 s of initiation of polymerization to cross-link and stabilize filaments, and any other structures that

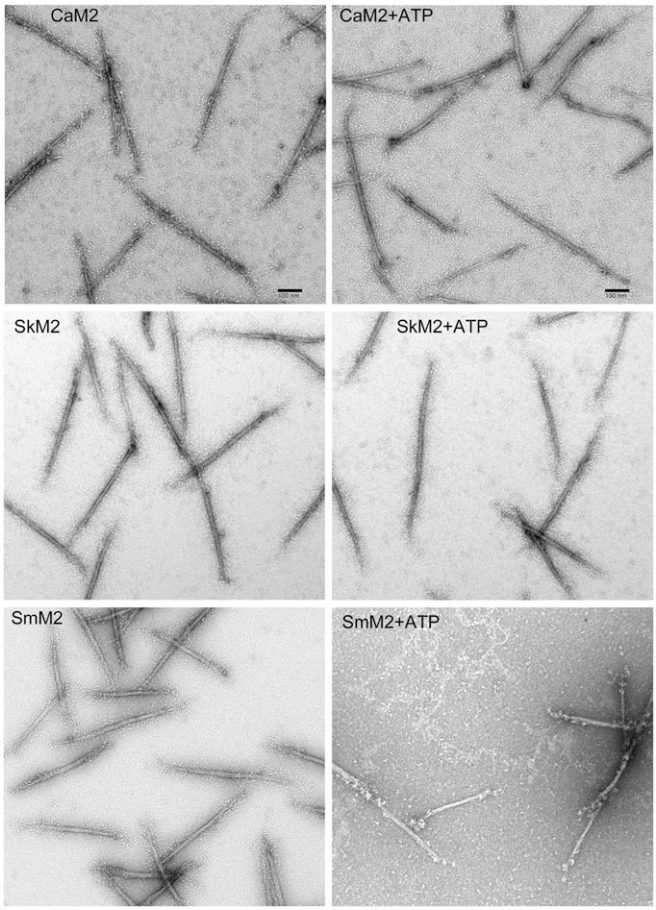

Fig. 2. Electron microscopy field images of filaments of CaM2, SkM2, and unphosphorylated SmM2 polymerized for 4 h in 150 mM NaCl, 2 mM $MgCl_2$, 1 mM DTT, and 10 mM Mops (pH 7.0) in the absence and presence of 1 mM ATP. Filaments were cross-linked for 30 min with 0.1 mM EDC before negative staining electron microscopy. (Scale bars: 100 nm.)

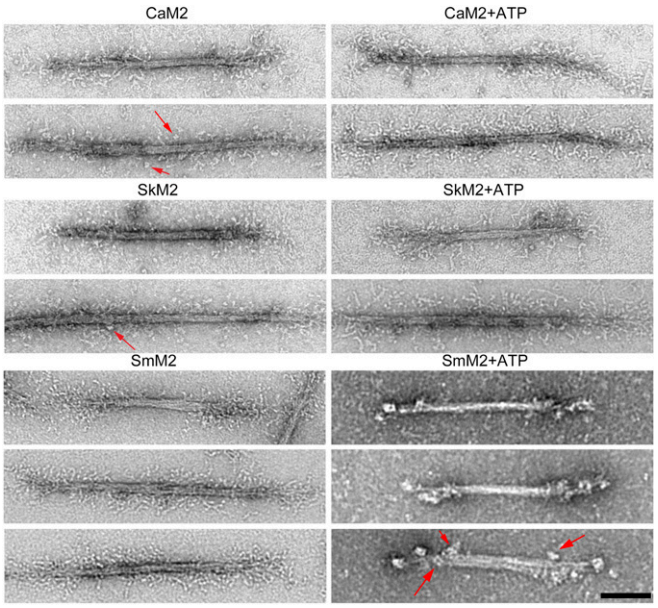

Fig. 3. Electron microscopy of individual filaments of CaM2, SkM2, and SmM2 polymerized for 4 h and prepared for analysis as in Fig. 2. CaM2 and SkM2 formed bipolar filaments with (*Upper*) and without (*Lower*) bare zones in both the presence and absence of ATP. In the absence of ATP, SmM2 formed bipolar filaments with (*Top*) and without (*Middle*) a bare zone and side-polar filaments (*Bottom*). In the presence of ATP, SmM2 formed only bipolar filaments. Red arrows identify clusters of four heads. (Scale bar: 100 nm.)

might be present, when the samples were diluted for negative staining electron microscopy. Glutaraldehyde was used rather than 1-ethyl-3-(3-dimethylaminopropyl-carbodiimide (EDC) because the former requires only 1 min for fixation (26) while the latter requires 30 min (27). Glutaraldehyde was an effective and necessary stabilizer. Light scattering remained constant when glutaraldehyde-fixed filaments were placed in 600 mM NaCl, which totally depolymerized nonglutaraldehyde-treated samples (*SI Appendix*, Fig. S1).

Field images of the polymerizing myosins at 4 s are shown in Fig. 5 and individual structures at higher magnification in Figs. 6–8. CaM2 and SkM2 in the absence of ATP and non-RLC–phosphorylated SmM2 with and without ATP formed tail-folded monomers, tail-folded antiparallel dimers, and tail-folded and partially unfolded antiparallel tetramers within ~4 s (Figs. 5 and 6). The tail-folded monomers of SkM2 and CaM2 and SmM2 were in the 10S conformation in the absence of ATP although the IHM was not observed in their head domains, whereas some of the folded SmM2 monomers in the presence of ATP did show IHMs (Fig. 6). Importantly, neither unfolded nor partially unfolded monomers and only a rare tail-folded parallel dimer was observed in any of the preparations.

Also, after polymerization, for only ~4 s, partially unfolded antiparallel tetramers of varied lengths, but no unfolded antiparallel dimers, were associated with elongating filaments (Fig. 7). The growing filaments in Fig. 7 show images of four heads (red arrows), three heads (blue arrows), presumably a tetramer with one head blocked (blue arrows), and filament-associated folded tetramers (yellow arrows). About 88%, 82%, and 75% of growing filaments of CaM2, SkM2, and SmM2, respectively, did not have clean bare zones, but their bare zones were associated with short folded structures, some of which were identified as folded tetramers. About 17%, 13%, and 13% of growing filaments of CaM2, SkM2, and SmM2, respectively, showed overlapping filaments (Fig. 5, yellow arrows and Fig. 8, green arrows), some clearly with four heads (Fig. 8, red arrow). None of these observations was an artifact of cross-linking by glutaraldehyde fixation as shown by their occurrence in nonfixed samples (*SI Appendix*, Fig. S2), although at lower concentrations probably because of partial depolymerization in the absence of fixation when the samples were diluted for electron microscopy.

Formation of Folded Structures during the Depolymerization of SmM2. Consistent with the higher critical concentration of non-RLC–phosphorylated SmM2 polymerized in the presence of ATP than in its absence (Fig. 1), addition of ATP rapidly depolymerizes filaments of non-RLC–phosphorylated SmM2 (28). Therefore, we added 50 μM ATP to filaments of non-RLC–phosphorylated SmM2 (Fig. 9*A*) that had been polymerized overnight in the absence of ATP, fixed the mixture with glutaraldehyde within ~4 s of addition of ATP to stop depolymerization, and identified depolymerizing structures by electron microscopy (Fig. 9*B*).

As if in the reverse of filament polymerization, depolymerizing long thick filaments formed overlapping thinner filaments (Fig. 9*B*, *1* and *2*, green arrows) and filaments with associated tail-folded tetramers (Fig. 9*B*, *3–6*, yellow arrows). We also observed individual folded antiparallel tetramers (Fig. 9*B*, T), tail-folded antiparallel dimers (Fig. 9*B*, D) and tail-folded monomers (Fig. 9*B*, M), but no unfolded monomers and only an occasional folded parallel dimer (Fig. 9*B*, PD). The heads of monomers, dimers, and tetramers were essentially all in the IHM conformation.

Discussion

Critical Concentrations. The data in Fig. 1 show that the critical concentrations of CaM2, SkM2, and SmM2 are similar to each other when polymerized in the absence of ATP, 4–7 nM, and also similar to the critical concentrations of mammalian nonmuscle myosin 2s, 3–10 nM (19), *Dictyostelium* myosin 2, 14 nM (29), and *Acanthamoeba* myosin 2, 5 nM (30). The critical concentrations of SkM2 and CaM2, which had not previously been reported, were only slightly higher when polymerized in the presence of ATP than when polymerized in the absence of ATP. The considerable increase in the critical concentration of non-RLC–phosphorylated SmM2 when polymerized in the presence

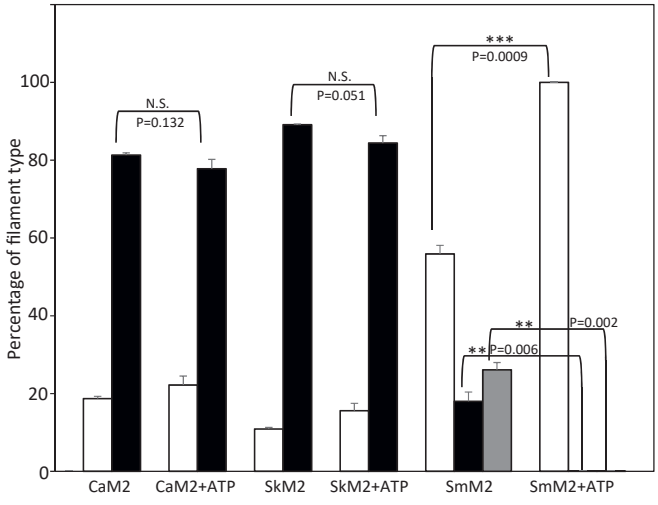

Fig. 4. Characterization by electron microscopy of CaM2, SkM2, and SmM2 filaments after polymerization for 4 h in the presence and absence of ATP. The percent of bipolar filaments with (white bar) and without (black bar) bare zones and side polar filaments (gray bar) were for more than 100 filaments in 20 fields of each of three sets each myosin polymerized as in Figs. 2 and 3. Data were from three separate preparations. Error bars in the figure denote SD. All data expressed as mean ± SD. Statistically significant (*P* value) was calculated using two tailed Student's *t* test. N.S., not significant ($P > 0.05$); $^{**}P \leq 0.01$; $^{***}P \leq 0.001$.

Table 1. Dimensions of filaments of SkM2, CaM2, and SmM2 polymerized for 4 h at room temperature with and without 1 mM ATP

	−ATP			+ATP		
	Filament length	Bare zone length	Filament width	Filament length	Bare zone length	Filament width
SkM2	580 ± 90 (n = 164)	69 ± 17 (n = 15)	18 ± 2 (n = 95)	576 ± 87 (n = 160)	92 ± 19 (n = 15)	18 ± 2 (n = 94)
CaM2	554 ± 90 (n = 128)	89 ± 17 (n = 42)	17 ± 2 (n = 128)	517 ± 91 (n = 100)	94 ± 18 (n = 50)	14 ± 3 (n = 132)
SmM2	507 ± 65 (n = 142)	101 ± 19 (n = 84)	18 ± 2 (n = 158)	373 ± 51 (n = 60)	187 ± 21 (n = 64)	15 ± 3 (n = 55)

The data were obtained from electron microscopic images of 15–164 negatively stained filaments, such as those shown in Figs. 2 and 3. Filament lengths and widths were calculated from all of the filaments and bare zone lengths only from the bipolar filaments that had bare zones (Fig. 4). Measurements were made using MetaMorph software.

of ATP, 117 nM, and the absence of ATP, 6 nM, was probably due to ATP inhibiting the unfolding of the folded tails of SmM2, which would be required for formation of filaments.

The critical concentrations we determined for SmM2 by light scattering are much lower than those determined by Kendrick-Jones et al. (18) by sedimentation at 100,000 × g for 20 min. This difference may be due to differences in the sensitivity of the methods used or to partial disassembly of myosin filaments polymerized in ATP during sedimentation (31).

Polymerization of Myosins. Contrary to our results, non-RLC–phosphorylated SmM2 had been thought to be unable to polymerize in the presence of ATP. In our study, polymerized filaments were cross-linked by either 0.1 mM EDC or 0.1 mM glutaraldehyde before application to the grid for negative staining. Cross-linking is required because otherwise filaments rapidly and partially disassemble when diluted for electron microscopy. The absence of cross-linking before electron microscopy may explain previous failures to obtain filaments of non-RLC–phosphorylated SmM2 polymerized in the presence of ATP.

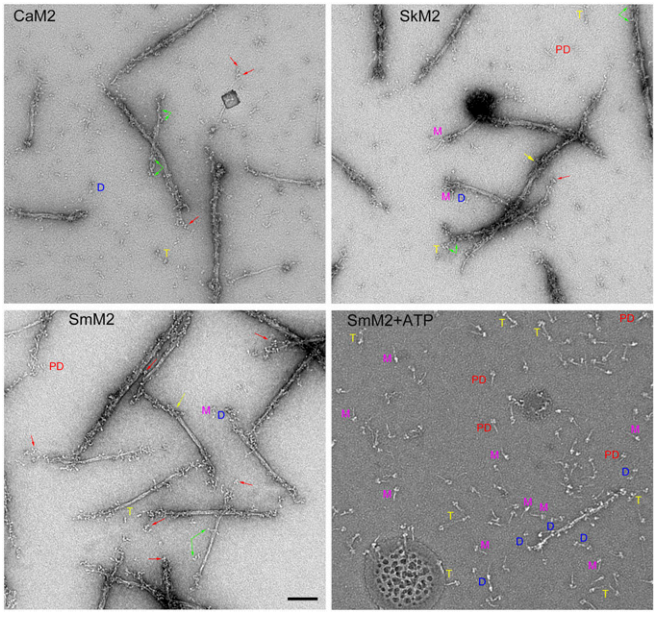

Fig. 5. Electron microscopy field images of CaM2, SkM2, and SmM2 polymerized for 4 s in 150 mM NaCl, 2 mM $MgCl_2$, 1 mM DTT and 10 mM Mops (pH 7.0) without and with 1 mM ATP (SmM2). Filaments were cross-linked for 1 min with 0.1 mM glutaraldehyde before negative staining electron microscopy. M, D, PD, and T stand for folded monomer, folded antiparallel dimer, folded parallel dimer, and folded antiparallel tetramer, respectively. Red arrows indicate a cluster of four heads, green arrows association of folded tetramers with growing filaments, and yellow arrows overlapping of growing filaments. (Scale bar: 100 nm.)

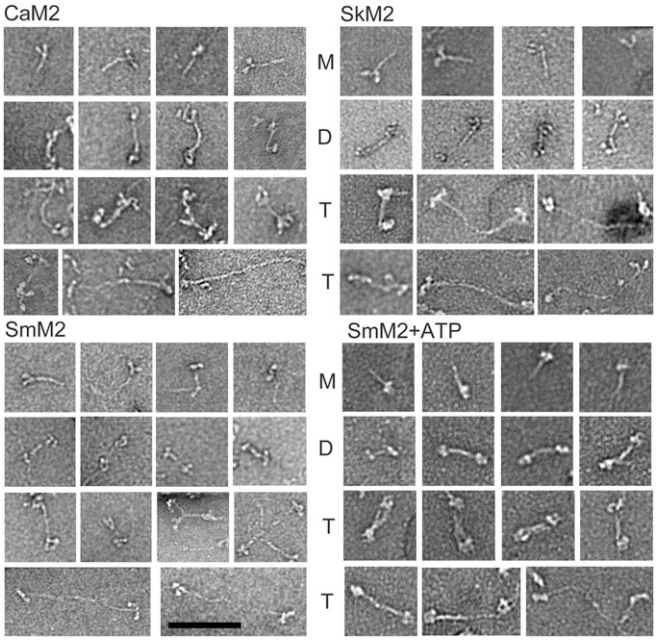

Fig. 6. Folded monomers, dimers, and tetramers of CaM2, SkM2, and SmM2 formed during polymerization for ~4 s. SkM2 and CaM2 were polymerized in the same buffer as in Fig. 2 without ATP, and SmM2 was polymerized in the same buffer both with and without 1 mM ATP. Images show folded monomers (M), folded dimers (D), and folded and partially unfolded tetramers (T). (Scale bar: 100 nm.)

The current models for polymerization of MM2s assume that folded 10S monomers are unable to polymerize. In these models, SkM2 and CaM2 monomers remain unfolded in the presence of ATP and 150 mM NaCl, whereas SmM2 forms folded 10S monomers that must be unfolded by RLC phosphorylation to enable polymerization. To the contrary, we find that SkM2, CaM2, and nonphosphorylated SmM2 form tail-folded monomers under polymerization conditions in vitro that associate into tail-folded dimers and tetramers that unfold and polymerize into filaments. This is essentially the same pathway that we proposed for the polymerization in vitro of nonmuscle myosin 2s (20), but the possible application of this pathway to polymerization of muscle myosins in vivo requires future experimentation.

Depolymerization of SmM2 in vitro appears to be the reverse of polymerization as the same structures, tail-folded tetramers, dimers, and monomers, are observed in both. The proposed in vitro polymerization and depolymerization pathways are also supported by the absence of extended monomers and antiparallel dimers and the association of folded and partially unfolded antiparallel tetramers with both polymerizing and depolymerizing filaments.

Consistent with these proposed pathways for in vitro polymerization of muscle myosins, others have reported that RLC phosphorylation does not unfold SmM2 monomers in 1 mM MgATP and 150 mM KCl (21), that unphosphorylated SmM2 can polymerize in the presence of ATP as determined by sedimentation (18, 24, 25), and that low concentrations of NaCl enhance both the concentration of folded monomers and the

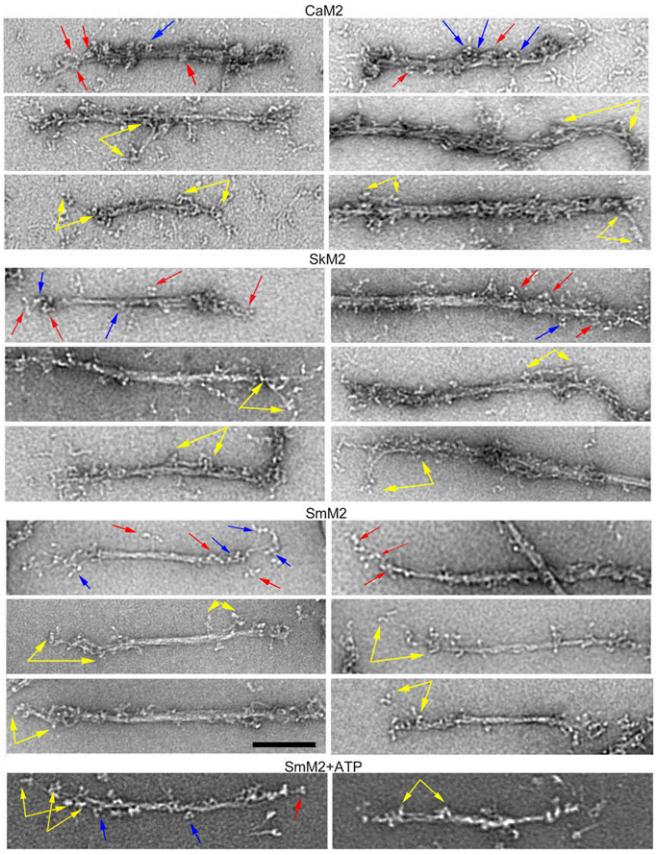

Fig. 7. Individual polymerizing filaments of CaM2, SkM2, and SmM2. Clusters of four heads (red arrows), three heads (blue arrows), and folded tetramers (yellow arrows) on polymerizing myosin filaments at ~4 s in the same buffer as in Fig. 2. (Scale bar: 100 nm.)

polymerization of CaM2 and SmM2 (25). Also, in a report on the in vitro polymerization of SmM2 (32), but not mentioned by the authors, one can see in figures 3 and 11D of ref. 32 association of folded tetramers and clusters of four heads with minifilaments. In the same paper (figure 11B of ref. 32), depolymerization (for an unspecified time) of dephosphorylated SmM2 minifilaments by addition of 1 mM MgATP was reported to form a mixture of tail-folded monomers, tail-folded antiparallel dimers, and tail-folded tetramers (not mentioned by authors) but no unfolded structures.

We speculate that the unfolded tetramers formed in the in vitro polymerization of muscle myosins may correspond to the subfilaments identified in crustacean muscle by X-ray diffraction (33) and in frozen-hydrated tarantula thick filament backbone by three-dimensional (3D) reconstruction mapping (34). The tarantula thick filament backbone consists of 12 uniform subfilaments. These subfilaments are ~4 nm in diameter, i.e., about twice the width of the coiled-coil tail of the myosin (~2 nm). Thus, it is more plausible that these subfilaments contain two, not three, myosin tails as had been suggested (33). Furthermore, folded tetramers can form by unfolding uniform subfilaments as shown by X-ray diffraction and 3D reconstruction (33, 34).

Recent 2-nm resolution 3D reconstruction of tarantula thick filaments shows that crowns of four myosin heads protrude above the thick filament backbone forming stable tandems of IHMs (35). This suggests that two myosin molecules must be closely spaced on the backbone so that they may intermolecularly interact. The closely spaced four heads as a group in tail-folded tetramers and unfolded tetramers in growing filaments shown in Figs. 6 and 7 may well fit the modeled IHMs (14, 35). Our data are also consistent with an early study (36) of native vertebrate skeletal muscle thick filaments by rotary shadow electron microscopy in which, although not mentioned by the authors, Fig. 1 shows multiple clusters of four heads protruding from the backbone of thick filaments. Equally important, the tail-folded tetramer demonstrated in this study as the principal polymerization unit in the rapid polymerization process in vitro might, in the presence of myosin-associated proteins, be the structural basis required for the formation of stable IHMs for each myosin molecule in thick filaments in vivo.

Why Tail-Folded Myosins? The interacting head and folded tail motifs of myosin monomers have been conserved since before the origin of animals (37–39). Heavy chain sequence analyses show that muscle and nonmuscle myosins are not closely related and their separation occurred at least 600 million years ago (39). Therefore, the highly conserved folded conformations of myosins must be of fundamental importance.

Folded monomers may be more efficient than extended monomers for myosin storage and transport in situ. Also, a polymerization pathway in which multiple folded tetramers unfold and polymerize into filaments may be more efficient than sequential addition of extended monomers.

Conclusion

We have shown that during their polymerization in vitro, skeletal, cardiac, and smooth muscle myosins form tail-folded monomers, dimers, and tetramers and that unfolded tetramers are probably the principal polymerization entity. Although we do not know whether polymerization of muscle myosins in vivo follows the proposed pathway for their polymerization in vitro, our results could help understand the polymerization process in vivo. Folded monomers and folded dimers have been observed in vivo, but folded tetramers have not been reported to be present in vivo. Also, polymerization in vivo may be affected by myosin-associated proteins, which include M-proteins, titin and myosin-binding protein C for SkM2 and CaM2, and smitin and

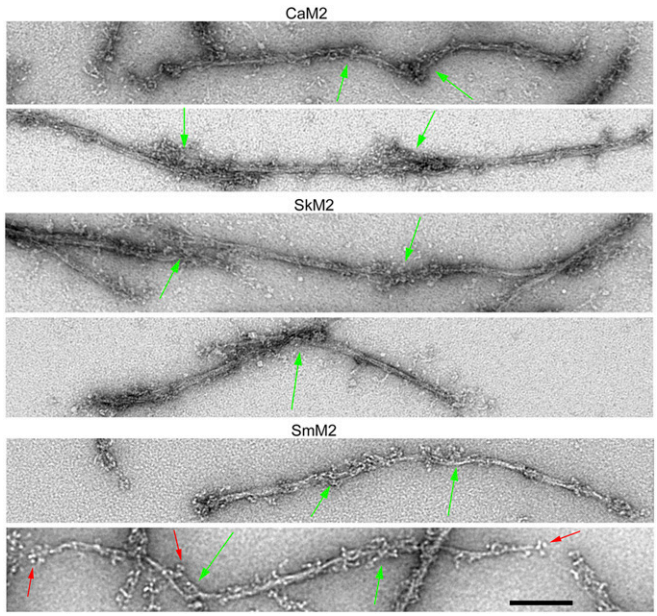

Fig. 8. Growing filaments overlap during the polymerization of CaM2, SkM2, and SmM2. Samples were taken after polymerization for ~4 s as in Fig. 5. Overlapping filaments (green arrows) and clusters of four heads (red arrows) are identified. (Scale bar: 100 nm.)

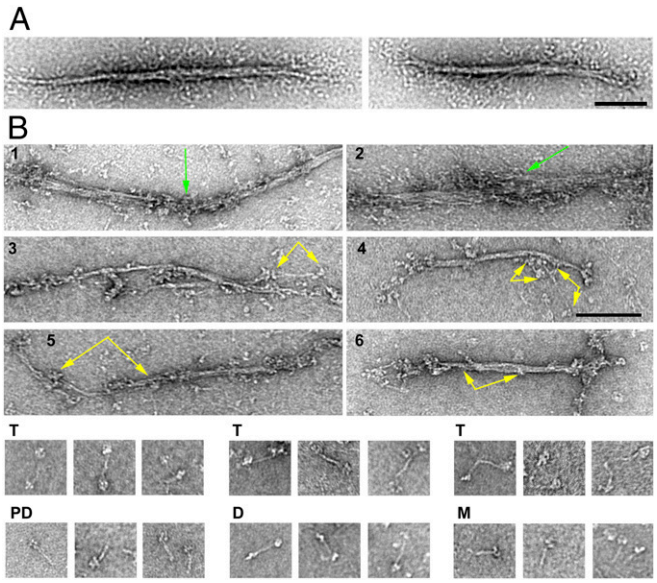

Fig. 9. Depolymerization of SmM2 is the reverse of polymerization. (*A*) Filaments polymerized without ATP, as in Fig. 2, but overnight to ensure complete polymerization, were a mixture of bipolar filaments without or with bare zones and side-polar filaments. (*B*) Images of filaments depolymerizing ∼4 s after addition of 50 μM ATP and cross-linked with 0.1 mM glutaraldehyde. *1* and *2* show overlapping filaments (green arrows); *3*–*6* show folded and partially folded tetramers (yellow arrows) associated with depolymerizing filaments; Individual folded tetramers (T), folded dimers (D), and folded monomers (M) also exist ∼4 s after depolymerization. Occasional folded parallel dimers (PD) were present, but no unfolded monomers were seen. (Scale bars: 100 nm.)

telokin for SmM2 (40). The possible effects of myosin-binding proteins on the polymerization of muscle myosins could be studied in vitro.

Materials and Methods

Myosins. Chicken gizzard smooth muscle myosin was the kind gift of Mitsuo Ikebe's laboratory, University of Texas Health Science Center, Tyler, TX. Rabbit skeletal muscle myosin and calf cardiac myosin were purchased from Cytoskeleton Inc.

Protein Concentration and Electrophoretic Assays. Protein concentrations were determined using the Bradford reagent (Bio-Rad) with purified myosin as the standard. The myosin standard concentration was determined by ultraviolet (UV) absorbance (myosin (mg/mL) = $(A_{280}–A_{260})/0.5$).

Light Scattering Assay of Muscle Myosin Polymerization. Myosin monomers in 600 mM NaCl were cleared by centrifugation at 300,000 × *g* for 15 min at 4 °C in a Beckman TL-100 centrifuge before use. Myosins were polymerized overnight on ice after dilution in 10 mM Mops (pH 7.0), 150 mM NaCl, 2 mM $MgCl_2$, 1 mM DTT, and 0.1 mM EGTA with and without 1 mM ATP. The samples were warmed to room temperature for 30 min, and light scattering was measured at 20 °C in a PTI fluorimeter. Excitation was performed at 365 nm (slit width 0.5 nm) and detection at 365 nm (slit width 0.5 nm). Data are the average of two assays.

Polymerization and Depolymerization Assays. Myosin monomers in 600 mM NaCl were cleared before use by centrifugation at 300,000 × *g* for 15 min at 4 °C in a Beckman TL-100 centrifuge. Myosins were polymerized in 10 mM Mops (pH 7.0), 150 mM NaCl, 2 mM $MgCl_2$, 1 mM DTT, and 0.1 mM EGTA without or with 1 mM ATP and were fixed immediately (∼4 s) by incubation for 1 min with 0.1 mM glutaraldehyde in assembly buffer at room temperature. The cross-linking reaction was stopped after 1 min by adding a 10% volume of 1 M Tris (pH 8.0) buffer.

Depolymerization of SmM2 filaments was induced by addition of 1 mM ATP in assembly buffer, to a final concentration of 50 μM, to filaments polymerized overnight in assembly buffer without ATP. Depolymerization was stopped at ∼4 s by glutaraldehyde fixation for 1 min at room temperature.

CaM2, SkM2, and SmM2 were also polymerized for 4 h and overnight in assembly buffer with and without 1 mM ATP. Prior to being applied to the grid for electron microscopy, the mature filaments were fixed with 0.1 mM EDC for 30 min at room temperature.

Electron Microscopy. After fixation by 0.1 mM glutaraldehyde for 1 min (24) or 0.1 mM EDC for 30 min (26), samples were diluted to about 200 nM myosin, and 4 μL were applied to a UV light-pretreated carbon-coated copper grid and stained with 1% uranyl acetate. Micrographs were recorded on a JEOL 1200EX II microscope at room temperature. Filament widths and lengths were determined with Metamorph software.

Data Availability. All relevant data, associated protocols, and materials are in the paper and *SI Appendix*.

ACKNOWLEDGMENTS. We are grateful to Dr. Mitsuo Ikebe for providing us with isolated chicken gizzard smooth muscle myosin and to Dr. James R. Sellers for his very useful suggestions during this research. We thank the Electron Microscope and Biophysics Cores of the National Heart, Lung and Blood Institute (NHLBI) for use of their facilities and the support of the NHLBI Division of Intramural Research.

1. J. R. Sellers, Myosins: A diverse superfamily. *Biochim. Biophys. Acta* **1496**, 3–22 (2000).
2. H. E. Huxley, Electron microscopic studies on the structure of natural and synthetic protein filaments from striated muscle. *J. Mol. Biol.* **7**, 281–308 (1963).
3. H. E. Huxley, The mechanism of muscular contraction. *Science* **164**, 1356–1365 (1969).
4. R. Craig, J. Megerman, Assembly of smooth muscle myosin into side-polar filaments. *J. Cell Biol.* **75**, 990–996 (1977).
5. H. Hinssen, J. D'Haese, J. V. Small, A. Sobieszek, Mode of filament assembly of myosins from muscle and nonmuscle cells. *J. Ultrastruct. Res.* **64**, 282–302 (1978).
6. T. D. Pollard, Electron microscopy of synthetic myosin filaments. Evidence for cross-bridge. Flexibility and copolymer formation. *J. Cell Biol.* **67**, 93–104 (1975).
7. C. Moos, G. Offer, R. Starr, P. Bennett, Interaction of C-protein with myosin, myosin rod and light meromyosin. *J. Mol. Biol.* **97**, 1–9 (1975).
8. J. F. Koretz, Structural studies of synthetic filaments prepared from column-purified myosin. *Biophys. J.* **27**, 423–432 (1979).
9. B. Kaminer, E. Szonyi, C. D. Belcher, "Hybrid" myosin filaments from smooth and striated muscle. *J. Mol. Biol.* **100**, 379–386 (1976).
10. H. Onishi, T. Wakabayashi, Electron microscopic studies of myosin molecules from chicken gizzard muscle I: The formation of the intramolecular loop in the myosin tail. *J. Biochem.* **92**, 871–879 (1982).
11. K. M. Trybus, T. W. Huiatt, S. Lowey, A bent monomeric conformation of myosin from smooth muscle. *Proc. Natl. Acad. Sci. U.S.A.* **79**, 6151–6155 (1982).
12. H. S. Jung, S. Komatsu, M. Ikebe, R. Craig, Head-head and head-tail interaction: A general mechanism for switching off myosin II activity in cells. *Mol. Biol. Cell* **19**, 3234–3242 (2008).
13. R. Craig, R. Smith, J. Kendrick-Jones, Light-chain phosphorylation controls the conformation of vertebrate non-muscle and smooth muscle myosin molecules. *Nature* **302**, 436–439 (1983).
14. L. Alamo *et al.*, Lessons from a tarantula: New insights into muscle thick filament and myosin interacting-heads motif structure and function. *Biophys. Rev.* **9**, 461–480 (2017).
15. R. L. Anderson *et al.*, Deciphering the super relaxed state of human β-cardiac myosin and the mode of action of mavacamten from myosin molecules to muscle fibers. *Proc. Natl. Acad. Sci. U.S.A.* **115**, E8143–E8152 (2018).
16. S. Yang *et al.*, The central role of the tail in switching off 10S myosin II activity. *J. Gen. Physiol.* **151**, 1081–1093 (2019).
17. K. M. Trybus, Assembly of cytoplasmic and smooth muscle myosins. *Curr. Opin. Cell Biol.* **3**, 105–111 (1991).
18. J. Kendrick-Jones, R. C. Smith, R. Craig, S. Citi, Polymerization of vertebrate non-muscle and smooth muscle myosins. *J. Mol. Biol.* **198**, 241–252 (1987).
19. X. Liu *et al.*, Effect of ATP and regulatory light-chain phosphorylation on the polymerization of mammalian nonmuscle myosin II. *Proc. Natl. Acad. Sci. U.S.A.* **114**, E6516–E6525 (2017).
20. X. Liu, S. Shu, E. D. Korn, Polymerization pathway of mammalian nonmuscle myosin 2s. *Proc. Natl. Acad. Sci. U.S.A.* **115**, E7101–E7108 (2018).
21. K. M. Trybus, S. Lowey, Conformational states of smooth muscle myosin. Effects of light chain phosphorylation and ionic strength. *J. Biol. Chem.* **259**, 8564–8571 (1984).
22. R. J. Ankrett, A. J. Rowe, R. A. Cross, J. Kendrick-Jones, C. R. Bagshaw, A folded (10 S) conformer of myosin from a striated muscle and its implications for regulation of ATPase activity. *J. Mol. Biol.* **217**, 323–335 (1991).
23. T. Katoh, K. Konishi, M. Yazawa, Skeletal muscle myosin monomer in equilibrium with filaments forms a folded conformation. *J. Biol. Chem.* **273**, 11436–11439 (1998).
24. T. Takahashi, C. Fukukawa, C. Naraoka, T. Katoh, M. Yazawa, Conformations of vertebrate striated muscle myosin monomers in equilibrium with filaments. *J. Biochem.* **126**, 34–40 (1999).

25. D. L. Milton *et al*., Direct evidence for functional smooth muscle myosin II in the 10S self-inhibited monomeric conformation in airway smooth muscle cells. *Proc. Natl. Acad. Sci. U.S.A.* **108**, 1421–1426 (2011).
26. N. Billington, A. Wang, J. Mao, R. S. Adelstein, J. R. Sellers, Characterization of three full-length human nonmuscle myosin II paralogs. *J. Biol. Chem.* **288**, 33398–33410 (2013).
27. E. Reisler, P. Cheung, C. Oriol-Audit, J. A. Lake, Growth of synthetic myosin filaments from myosin minifilaments. *Biochemistry* **21**, 701–707 (1982).
28. H. Suzuki, T. Kamata, H. Onishi, S. Watanabe, Adenosine triphosphate-induced reversible change in the conformation of chicken gizzard myosin and heavy meromyosin. *J. Biochem.* **91**, 1699–1705 (1982).
29. E. R. Kuczmarski, J. A. Spudich, Regulation of myosin self-assembly: Phosphorylation of *Dictyostelium* heavy chain inhibits formation of thick filaments. *Proc. Natl. Acad. Sci. U.S.A.* **77**, 7292–7296 (1980).
30. J. H. Sinard, T. D. Pollard, The effect of heavy chain phosphorylation and solution conditions on the assembly of *Acanthamoeba* myosin-II. *J. Cell Biol.* **109**, 1529–1535 (1989).
31. J. S. Davis, The influence of pressure on the self-assembly of the thick filament from the myosin of vertebrate skeletal muscle. *Biochem. J.* **197**, 301–308 (1981).
32. K. M. Trybus, S. Lowey, Assembly of smooth muscle myosin minifilaments: Effects of phosphorylation and nucleotide binding. *J. Cell Biol.* **105**, 3007–3019 (1987).
33. J. S. Wray, Structure of the backbone in myosin filaments of muscle. *Nature* **277**, 37–40 (1979).
34. J. L. Woodhead *et al*., Atomic model of a myosin filament in the relaxed state. *Nature* **436**, 1195–1199 (2005).
35. L. Alamo *et al*., Conserved intramolecular interactions maintain myosin interacting-heads motifs explaining tarantula muscle superrelaxed state structural basis. *J. Mol. Biol.* **428**, 1142–1164 (2016).
36. J. Trinick, A. Elliott, Electron microscope studies of thick filaments from vertebrate skeletal muscle. *J. Mol. Biol.* **131**, 133–136 (1979).
37. H. S. Jung *et al*., Conservation of the regulated structure of folded myosin 2 in species separated by at least 600 million years of independent evolution. *Proc. Natl. Acad. Sci. U.S.A.* **105**, 6022–6026 (2008).
38. K. H. Lee *et al*., Interacting-heads motif has been conserved as a mechanism of myosin II inhibition since before the origin of animals. *Proc. Natl. Acad. Sci. U.S.A.* **115**, E1991–E2000 (2018).
39. K. J. Peterson *et al*., Estimating metazoan divergence times with a molecular clock. *Proc. Natl. Acad. Sci. U.S.A.* **101**, 6536–6541 (2004).
40. R. Craig, J. L. Woodhead, Structure and function of myosin filaments. *Curr. Opin. Struct. Biol.* **16**, 204–212 (2006).